Molecular mechanism of C-reaction protein in promoting migration and invasion of hepatocellular carcinoma cells *in vitro*

SHASHA SHEN[1*], JIAOJIAO GONG[1*], YIXUAN YANG[1], SI QIN[1], LIFAN HUANG[1], SHA SHE[1], MIN YANG[1], HONG REN[1] and HUAIDONG HU[1,2]

[1]Key Laboratory of Molecular Biology for Infectious Diseases (Ministry of Education), Institute for Viral Hepatitis, Department of Infectious Diseases, The Second Affiliated Hospital, Chongqing Medical University, Chongqing; [2]Department of Clinical Nutrition, The Second Affiliated Hospital of Chongqing Medical University, Chongqing, P.R. China

Received January 5, 2017; Accepted March 7, 2017

DOI: 10.3892/ijo.2017.3911

Abstract. Hepatocellular carcinoma (HCC) is one of most common malignant cancers and is the second leading cause of cancer related deaths. The prognosis and survival of patients are closely related to the degree of tumor metastasis. The mechanism of HCC metastasis is still unclear. In the present study, we investigated the molecular mechanism of C-reaction protein in promoting migration and invasion of hepatocellular carcinoma cells *in vitro*. We estimated that CRP is overexpressed in liver cancer tissues and that it promotes invasion and metastasis of HCC *in vitro*. In the present study, we employed iTRAQ-based mass spectrometry to analyze the HepG2 secretory proteins of CRP siRNA-treated cells and negative control siRNA-treated cells. We identified 109 differentially expressed proteins after silencing CRP, of which 45 were upregulated and 64 were downregulated. Some of the differentially expressed proteins were confirmed by western blot analysis and real-time quantitative PCR. Furthermore, we found that knockdown of CRP substantially abrogates HIF-1α expression levels, the luciferase activity of HIF-1α and ERK and Akt phosphorylation in HepG2 cells. The present study provides a novel mechanism by which CRP promotes the proliferation, migration, invasion and metastasis of hepatocellular carcinoma cells. Inhibition of CRP suppressed migration, invasion and healing of hepatoma carcinoma cells by decreasing HIF-1α activity and CTSD.

Correspondence to: Dr Huaidong Hu, Key Laboratory of Molecular Biology for Infectious Diseases (Ministry of Education), Institute for Viral Hepatitis, Department of Infectious Diseases, The Second Affiliated Hospital, Chongqing Medical University, Chongqing 400010, P.R. China
E-mail: huhuaidong@sina.com

*Contributed equally

Key words: C-reactive protein, hepatocellular carcinoma, iTRAQ, HIF-1α, CTSD

Introduction

Hepatocellular carcinoma (HCC) is the fifth most common malignant cancer and the second leading cause of cancer related deaths globally (1,2). Despite the improvement of surgical techniques and adjuvant therapies, approximately 20% of HCC patients still suffer extra-hepatic metastases within 5-10 years of receiving radical surgical treatment. The long-term survival of patients with metastases remains low (3). Therefore, it is critical to discover the mechanisms underlying HCC metastasis.

C-reactive protein (CRP), a prototypic acute-phase protein and a member of the ancient and highly conserved proteins of the pentraxin family, has a cyclic pentameric structure. CRP is involved directly in a wide range of inflammatory processes and contributes to innate host immunity (4). Moreover, CRP is a sensitive systemic marker of inflammation and tissue damage. Elevated levels of CRP are detected in patients with infections, inflammatory diseases, or necrosis (5). Upregulation of CRP expression has been implicated in many types of tumors, including ovarian (6), lung (7), colon cancer (8), multiple myeloma (9) and lymphoma (10). Previous studies focused mostly on the expression level of CRP in cancer patients. Several studies have demonstrated that CRP promotes cell proliferation in endothelial cells, endothelial progenitor cells, renal tubular epithelial cells, and protects against apoptosis in myeloma cells (11,12), which are implicated in tumorigenesis and the development of HCC. Despite evidence of CRP being involved in a variety of cancers, the role of CRP in regulating HCC metastasis remains unclear.

Recently, the use of isobaric tags for relative and absolute quantitation (iTRAQ) technology has become a particularly powerful tool and has been recommended by the proteomics community to enable deeper proteome coverage, since it can facilitate simultaneous analysis of up to eight samples in one experiment. The aim of the present study was to use iTRAQ to identify alterations in the proteome of CRP siRNA treated samples, compared to control samples, in order to identify proteins participating in the migration and invasion of HCC.

In the present study, we hypothesized that CRP has an effect on invasion and metastasis of HCC. To elucidate the potential mechanism/pathway by which CRP contributes to

migration and invasion, iTRAQ-based MS was performed to analyze differentially expressed proteins (DEPs) between the supernatants of CRP siRNA-treated supernatant and the negative siRNA-treated HepG2 cells.

Materials and methods

Immunohistochemistry (IHC) and tissue microarrays (TMA). A commercial tissue microarray (BC03117; Us Biomax, Inc., Rockville, MD, USA), containing 40 cases of hepatocellular carcinoma and 40 matched cancer adjacent normal tissues, was used for IHC evaluation of CRP. Liver sections embedded in paraffin were deparaffinized in xylene, rehydrated in ethanol and washed in double-distilled H_2O (13). Endogenous peroxidase activity was quenched by incubating the sections for 10 min in 3% H_2O_2, and the liver sections were then blocked with BSA for 30 min. The sections were incubated with primary antibodies against CRP (1:100 dilution) overnight at 4˚C. IHC visualization of CRP was performed with an EnVision system with horseradish peroxidase (Dako Cytomation, Glostrup, Denmark) (13).

Cell lines. Human HCC cell lines, HepG2 (ATCC, Manassas, VA, USA) and the BEL7402 (Cell Bank of the Chinese Academy of Medical Science, Beijing, China), were cultured in an atmosphere of 5.0% carbon dioxide at 37˚C in RPMI-1640 medium that was supplemented with 10% fetal bovine serum (FBS; Gibco, San Diego, CA, USA) and 100 IU/ml penicillin.

CRP siRNA transfection, Transwell assays and wound healing. HepG2 and BEL7402 cells were transfected with 100 nM of CRP specific Stealth Select RNAi™ siRNA (sc-40816) or a negative control siRNA (12935-400) using Lipofectamine 2000 (Invitrogen, Carlsbad, CA, USA), following the manufacturer's instructions. After transfection for 6 h, the culture medium was replaced with fresh RPMI-1640, supplemented with 10% FBS and penicillin, and the cells continued in culture for an additional 42 h. To explore the role of CRP in the *in vitro* progression of HCC, wound-healing, cell migration and invasion assays were conducted two days after transfection. The wound healing assays were performed in 6-well plates. As the cell reached confluence, a wound was incised in the cell monolayer using a sterile p200 pipette tip, followed by three washes with medium. Digital images of the wound areas were captured after 0 and 24 h, using a phase contrast microscope. The Transwell invasion assays were performed using a 24-well Cell Invasion Assay kit (Cell Biolabs, Inc., San Diego, CA, USA). Briefly, HepG2 cells were harvested and re-suspended in serum-free media until they were transfected with CRP or control siRNA for 48 h. Approximately $2x10^5$ transfected cells were loaded into the upper chamber and 500 μl media (1640 plus 10% FBS) was loaded into the lower chambers. Cells were incubated for 24 h. The non-invasive cells were removed using cotton swabs, and the number of invading cells on the bottom of the filters were measured using CyQUANT GR fluorescent dye and detection at 560 nm. In each case, the silencing of CRP expression was verified by western blot analysis.

The HepG2 cell secretory proteins collection. Two days following HepG2 transfected with 100 nM of CRP specific Stealth Select RNAi™ siRNA (sc-40816) or a negative control siRNA, the culture medium was again replaced with fresh RPMI-1640 without FBS or penicillin and continued to culture for 2 days. Then the HepG2 cell culture medium without FBS or penicillin (secretory proteins) were concentrated and used for iTRAQ-coupled LC-MS/MS analyses.

ITRAQ labeling. The 8-plex iTRAQ kits were purchased from Applied Biosystems (Foster City, CA, USA). The secretory proteins was collected as described above and the protein concentrations were quantified by 2D Quant kit (Amersham Biosciences). Approximately 100 μg of protein from each sample was precipitated, dissolved in dissolution buffer, denatured, cysteine blocked, digested with 2 μg of sequencing grade modified trypsin and labeled using iTRAQ reagents as follows: negative control siRNA transfected protein, 113 and 116 tags; pooled CRP siRNA-treated protein, 115 and 117 tags: pooled negative siRNA-treated protein. The labeled samples were combined before analysis.

Peptide fractionation. The method of peptide fractionation was immobilized-pH-gradient isoelectric focusing (IPG-IEF), as previously described (14,15). Briefly, the pooled iTRAQ-labeled samples were solubilized in Pharmalyte (Amersham Biosciences) and 8 M urea, rehydrated on 18 cm-long IPG gel strips (pH 3-10; Amersham Biosciences), and then subjected to IEF focusing at 68 kV/h with an IPGphor System (GE Healthcare). Peptides were extracted by incubating the gel pieces in acetonitrile and formic acid. The pieces were purified and concentrated on a C18 Discovery DSC-18 SPE column (Sigma-Aldrich), lyophilized and stored at -20˚C until LC-MS/MS analysis.

Mass spectrometry. A QStar Elite mass spectrometer (Applied Biosystems) coupled with an Dionex UltiMate 3000 liquid chromatography system (Thermo Fisher Scientific, Amsterdam, The Netherlands) was used for mass spectrometric analysis (16). Peptide separation was carried out on a C18 analytical column (Thermo Fisher Scientific, Beijing, China). Purified peptide fractions were dissolved in buffer A (98% ACN), loaded onto a C18 trap column and subsequently eluted from the trap column over the C18 analytical column at a flow rate of 300 nl/min in 125 min linear gradient ranging from 2 to 100% mobile phase B (0.1% formic acid, 98% acetonitrile). Data acquisition was done in the positive ion mode, with a selected mass range of 300-1800 m/z. The two most abundantly charged ions which exceeded 20 counts were chosen for MS/MS at a dynamic exclusion of 30 sec (17). Protein identification and quantification were performed with ProteinPilot v2.0 (AB Sciex). MS/MS data were processed by searching the International Protein Index (IPI) human database v3.77. Methyl methane thiosulfate (MMTS) modified cysteine was specified as a fixed modification. Proteins having at least two unique peptides with fold-change >1.3 or <0.77 ($P<0.05$) between two stages were considered to be differentially expressed proteins.

Bioinformatics. Gene Ontology analysis was performed using PANTHER (http://www.pantherdb.org/) to classify biological processes, protein classes and molecular functions.

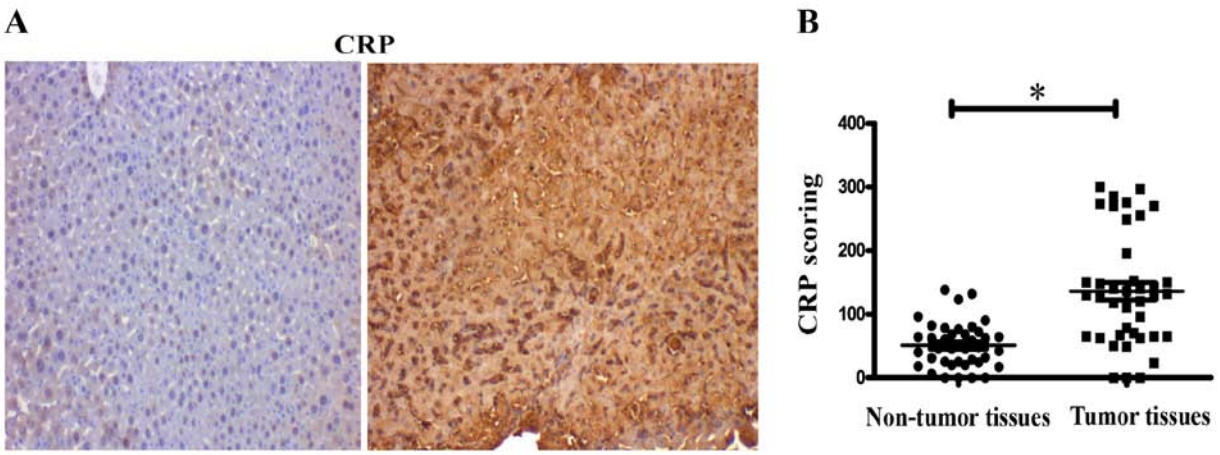

Figure 1. Immunohistochemical analysis of CRP proteins in tissue microarrays containing HCC tissues and adjacent non-cancerous tissues. (A) Representative images of the immmunohistochemical analysis of CRP in HCC tissue and adjacent non-cancerous tissues. (B) IHC score values of CRP are significantly higher in HCC tissue compared to matched HCC adjacent non-cancerous tissues. *P<0.05.

RNA extraction and quantitative RT-PCR. Total RNA was extracted from HepG2 cells with TRIzol reagent (Gibco-BRL, Gaithersburg, MD, USA), according to the manufacturer's instructions. First-strand cDNA was synthesized using a Thermo Scientific RevertiAid First Strand cDNA synthesis kit (Thermo Fisher Scientific). RT-PCR was performed on an ABI 7900HT system using the KAPA SYBR® FAST Universal 2X qPCR Master Mix and primers for GAPDH (Hs00486019_CE), GFAP (Hs00167550_CE), CUL1 (Hs00667710_CE), FAHD1 (Hs00636334_CE), NME2 (Hs00543451_CE), GNPDA2 (Hs00831453_CE), CALM2 (Hs00710519_CE), DDB1 (Hs00586106_CE), HSPD1 (Hs00830627_CE), CTSZ (Hs00664339_CE), CDH2 (Hs00805624_CE), IL11 (Hs00545902_CE), (Hs00829008_CE), NUCB1 (Hs00817382_CE), COL1A1 (Hs00747266_CE), SDF4 (Hs00796825_CE) and CSRP1 (Hs00723484_CE). The relative changes of gene expression were calculated according to the $2^{-\Delta\Delta CT}$ quantification method (18).

Western blotting. HepG2 cells were lysed with a non-ionic detergent (NID) lysis buffer. The resulting soluble cell extract was centrifuged for 30 min at 12,000 x g and the intracellular protein was collected. Additional, the secretory proteins was concentrated for 30 min at 3400 x g using an ultrafiltration centrifuge tube, after which the extracellular protein was collected. The intracellular and extracellular protein concentrations were determined using a 2-D Quant kit (GE Healthcare). Protein (40 μg) was separated by SDS-PAGE and transferred to PVDF membranes (Amersham Biosciences). Membranes were blocked for 1 h with 5% non-fat powdered milk in TBS-T buffer (pH 7.6, 0.5% Tween-20), then incubated overnight with primary antibodies at 4˚C. These monoclonal antibodies against CRP, CTSZ, IL11, CTSD, COL1A1, CUL1, CALM2, HIF-1α, p-AKT, AKT, p-ERK, ERK and actin (Abcam, Cambridge, MA, USA) were diluted from 1:2,000 to 1:10,000. After washing three times with TBS-T buffer, the membranes were incubated with a horseradish peroxidease-conjugated (HRP) goat anti-rabbit IgG or goat anti-mouse IgG (Santa Cruz Biotechnology) as the secondary antibody (1:5,000 dilution) for 1 h at room temperature. The membranes were washed again three times with TBS-T buffer and visualized with the ChemiDoc MP Imaging system (Bio-Rad Laboratories, Hercules, CA, USA).

The detection of HIF-1α luciferase activity. HepG2 cells transfected with either CRP siRNA or control siRNA were plated into 24-well plates. After 24 h of transfection, the HepG2 cells were co-transfected with 500 ng of plasmid pGL3 and 15 ng of pRL-SV40 using Lipofectamine 2000. After transfection for additional 24 h, the Luciferase activity of HIF-1α was determined on a GloMax 20/20 using the Dual-luciferase assay kit (Promega GmbH, Mannheim, Germany). Firefly luciferase units were normalized with *Renilla* luciferase carried by pRL-SV40 plasmid. Each experiment was performed in triplicate.

Statistical analysis. The experimental data are presented as the mean ± standard deviation (SD), and differences between the two groups were analyzed using the Student's t-test. P<0.05 was considered statistically significant. SPSS software v16.0 (SPSS, Inc., Chicago, IL, USA) was used for the analyses.

Results

Overexpression of CRP in hepatocellular carcinoma tissues. The expression of CRP was assessed in tissue microarrays, containing 40 cases of hepatocellular carcinoma and 40 matched adjacent normal tissue by IHC. IHC evaluation of tissue microarrays showed that expression of CRP was significantly stronger in tumor tissues than in normal tissues (P<0.05) (Fig. 1A). IHC score values of CRP were significantly higher in the HCC tissues than in the HCC adjacent normal tissues (P<0.05) (Fig. 1B).

CRP inhibits HCC cell migration, invasion and wound healing. To study the role of CRP in tumor cell motility, we used CRP-specific siRNA to silence CRP expression in HCC cell lines (HepG2 and BEL7402). Western blot analysis showed that CRP siRNA-treated cell lines downregulated CRP expression significantly (Fig. 2A). The invasion assay demonstrated

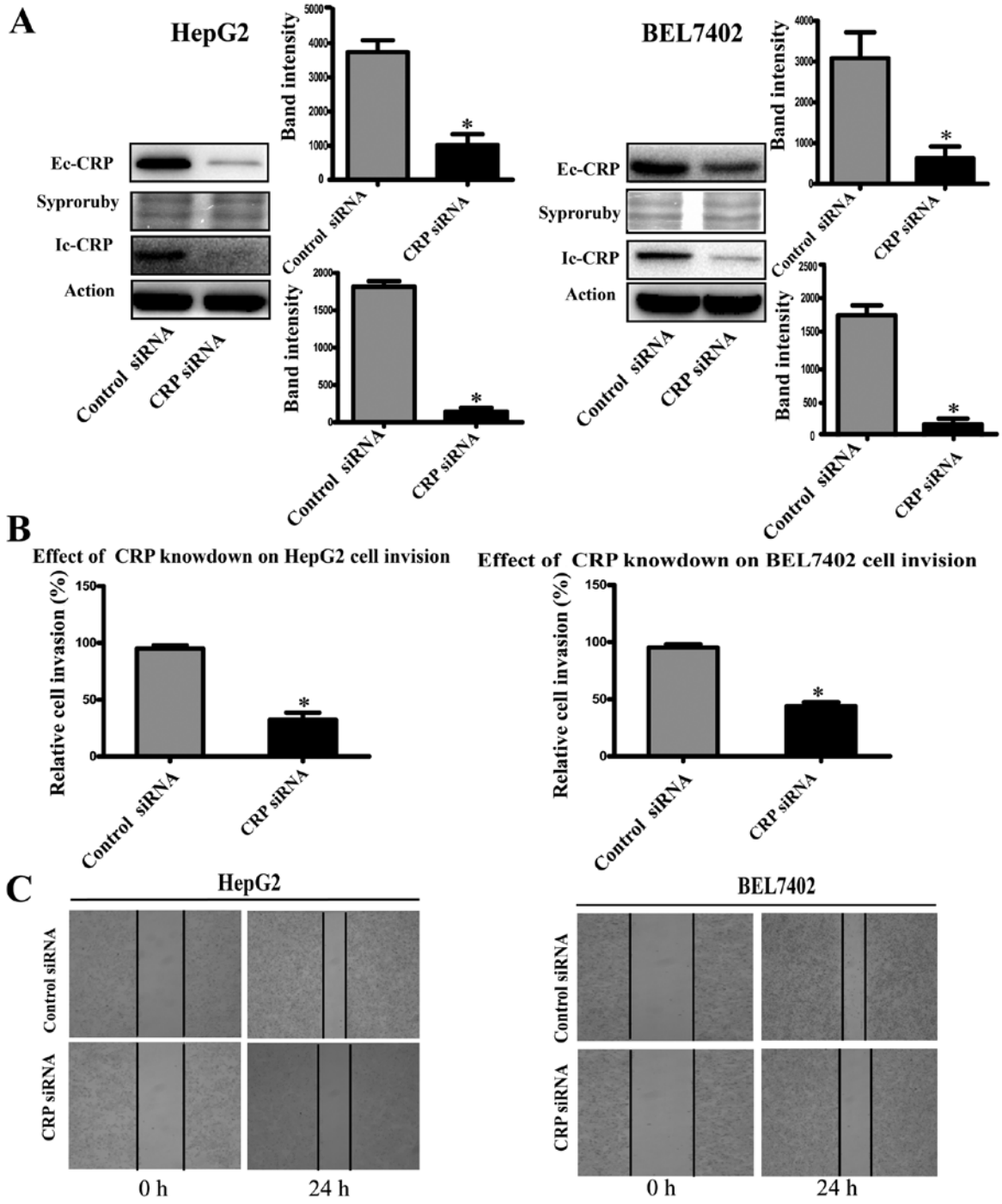

Figure 2. CRP plays important roles in the migration and invasion of HCC cells. (A) Cells were transfected with CRP-targeted siRNAs. Western blot analysis shows that the silencing of CRP significantly reduced CRP protein levels, intracellular CRP (Ic-CRP) and extracellular CRP (Ec-CRP) of HepG2 and BEL7402 cells. The respective gray scale analysis results are shown. (B) The invasion ability was significantly inhibited in CRP-knockdown cells. (C) Wound healing assays using CRP-knockdown cells (*P<0.05).

that the downregulation of CRP markedly weakened the migration and invasion capabilities of HepG2 and BEL7402 cells by 63 and 50%, respectively (P<0.05) (Fig. 2B). Similarly, the ability to close scratch wounds was decreased in HepG2 and BEL7402 cells (Fig. 2C).

Analysis of iTRAQ data of aberrantly expressed proteins. To investigate the molecular mechanism of CRP in the suppression of HCC migration and invasion, we conducted iTRAQ-based MS to analyze secretory proteins from CRP siRNA-treated and negative control siRNA-treated HepG2 cells. The ratio of 115:113 and 117:116 expressed the relative protein expression in the CRP siRNA-treated and negative control siRNA-treated secretory proteins. Hundreds of proteins were identified by ProteinPilot 2.0 software. The protein threshold was set to achieve 95% confidence at 5% FDR (false discovery rate). To define the differentially expressed proteins (DEPs), we introduced an additional ±1.3-fold cut-off for all iTRAQ ratios (19,20). Using this value, the overall data from technical replicate analyses produces <30% variation. A total of 401

Figure 3. PANTHER Classification System analysis of differentially expressed proteins in CRP-siRNA treated supernatant protein of HeG2 cells. Proteins were categorized by (A) biological process, (B) molecular function and (C) protein class.

unique proteins were confidently identified and quantified, regardless of whether the P-value was <0.05 in the iTRAQ ratios. Of the 109 proteins expressed differentially between the CRP siRNA-treated samples and the negative control siRNA-treated samples, 45 proteins were overexpressed and 64 were downregulated. The top 30 upregulated and downregulated proteins are shown in Table I.

Cellular and molecular functional characteristics of the differentially expressed proteins. To better identify the functional characteristics of the 109 DEPs, these proteins were grouped by PANTHER Classification System according to their reported biological process, protein class and molecular functions. Gene Ontology analysis with PANTHER suggested that the DEPs was found to represent a total of 11 biological processes, 20 protein classes and 6 molecular functions (Fig. 3). Metabolic, cellular and developmental processes were the most common biological processes reported.

Validation of differentially expressed proteins. To validate the reliability of the iTRAQ analysis data, we chose samples used in the iTRAQ assays and conducted western blotting and RT-PCR to detect the extracellular levels of several DEPs. Fig. 4A shows the relative mRNA expression levels of CTSZ, CDH2, IL11, CTSD, NUCB1, COL1A1, SDF4, CSRP1, HSPD1, GFAP, CUL1, FAHD1, NME2, CALM2, DDB1, and GNPDA2 as normalized to GADPH. RT-PCR showed the mRNA levels of CTSZ, CDH2, IL11, CTSD, NUCB1, COL1A1, SDF4, CSRP1 and HSPD1 were downregulated, whereas the mRNA levels of GFAP, CUL1, FAHD1, NME2, CALM2, DDB1 and GNPDA2 were upregulated in the CRP siRNA-treated samples, compared to the negative control

Table I. The top 30 upregulated and downregulated differentially expressed proteins, as identified using iTRAQ technology.

N	Accession	Gene symbol	Protein name	Peptides -95%	CRP knockdown: control (115:113)	PVal 115:113	CRP knockdown: control (117:116)	PVal 117:116
Top 30 proteins upregulated in CRP siRNA secretory protein								
1	sp|P14136|GFAP_HUMAN	GFAP	Glial fibrillary acidic protein	15	2.697659	0.009843	2.729757	0.010676
2	tr|J3QR68|J3QR68_HUMAN	HP	Haptoglobin	11	2.262996	0.002992	2.545902	0.002731
3	sp|P51884|LUM_HUMAN	BLMH	Bleomycin hydrolase	3	1.987454	0.039766	1.995493	0.046258
4	tr|A8K3S1|A8K3S1_HUMAN	GNPDA2	Glucosamine-6-phosphate isomerase	10	1.874345	0.006277	1.693967	0.030001
5	sp|P10155|RO60_HUMAN	TROVE2	60 kDa SS-A/Ro ribonucleoprotein isoform	8	1.810782	0.000753	1.685377	0.00063
6	tr|Q53GX6|Q53GX6_HUMAN	GSTO1	Highly similar to Homo sapiens glutathione S-transferase omega 1	4	1.794569	0.016479	1.71704	0.015401
7	tr|H0Y8C6|H0Y8C6_HUMAN	IPO5	Importin-5	27	1.661198	0.00088	1.677587	0.000784
8	tr|Q32Q12|Q32Q12_HUMAN	NME2	Nucleoside diphosphate kinase	54	1.660392	0.014814	1.723658	0.004326
9	tr|H0Y7A7|H0Y7A7_HUMAN	CALM2	Calmodulin	23	1.618516	0.014581	1.497814	0.048883
10	sp|Q6P587|FAHD1_HUMAN	FAHD1	Acylpyruvase FAHD1	6	1.597314	0.048898	1.745514	0.006089
11	tr|Q6LET3|Q6LET3_HUMAN	HPRT1	HPRT1 protein	12	1.561261	0.003935	1.6111	0.000739
12	tr|K7EKD8|K7EKD8_HUMAN	CAPNS1	Calpain small subunit 1	2	1.550796	0.050152	1.564854	0.057883
13	tr|A0A024R462 _HUMAN	FN1	Fibronectin 1	129	1.507385	4.96E-11	1.516702	3.37E-09
14	sp|Q13616|CUL1_HUMAN	CUL1	Cullin-1	4	1.468003	0.029943	1.863864	0.026399
15	sp|Q04760|LGUL_HUMAN	GLO1	Lactoylglutathione lyase	13	1.452267	0.018025	1.434937	0.010939
16	sp|P30041|PRDX6_HUMAN	PRDX6	Peroxiredoxin-6	28	1.438182	0.038665	1.523574	0.027196
17	sp|P26641|EF1G_HUMAN	EEF1G	Elongation factor 1-gamma	14	1.434626	0.025754	1.47196	0.020297
18	tr|B0YIW6|B0YIW6_HUMAN	ARCN1	Archain 1	7	1.432327	0.035547	1.374012	0.10264
19	sp|P55060|XPO2_HUMAN	CSE1L	Exportin-2	18	1.413718	0.009854	1.407874	0.025418
20	sp|O75436|VP26A_HUMAN	VPS26A	Vacuolar protein sorting-associated protein 26A	8	1.424428	0.042069	1.388839	0.022327
21	sp|P27695|APEX1_HUMAN	APEX1	DNA-(apurinic or apyrimidinic site) lyase	9	1.388838	0.031594	1.508206	0.008443
22	sp|P48637|GSHB_HUMAN	GSS	Glutathione synthetase	16	1.386073	0.020581	1.319895	0.000501
23	sp|Q16531|DDB1_HUMAN	DDB1	DNA damage-binding protein 1	35	1.370885	0.002909	1.491143	0.000105
24	tr|H7C2I1|H7C2I1_HUMAN	PRMT1	Protein arginine N-methyltransferase 1	10	1.369152	0.013057	1.446224	0.026285
25	sp|P60900|PSA6_HUMAN	PSMA6	Proteasome subunit alpha type-6	22	1.359674	0.007907	1.347712	0.034374
26	sp|Q13907|IDI1_HUMAN	IDI1	Isopentenyl-diphosphate Delta-isomerase 1	4	1.359607	0.030252	1.374364	0.105732
27	sp|Q8N543|OGFD1_HUMAN	OGFOD1	Prolyl 3-hydroxylase OGFOD1	5	1.351501	0.050466	1.353389	0.038133
28	sp|Q93009|UBP7_HUMAN	USP7	Ubiquitin carboxyl-terminal hydrolase 7	10	1.33261	0.020238	1.417985	0.135236
29	sp|P13639|EF2_HUMAN	EEF2	Elongation factor 2	48	1.324262	0.041668	1.352563	0.000136
30	tr|H0UID3|H0UID3_HUMAN	AP2B1	Adaptor-related protein complex 2	16	1.311697	0.003873	1.434811	0.014619

Table I. Continued.

N	Accession	Gene symbol	Protein name	Peptides -95%	CRP knockdown: control (115:113)	PVal 115:113	CRP knockdown: control (117:116)	PVal 117:116
Top 30 proteins downregulated in CRP siRNA secretory protein								
1	tr|B4E3Q1|B4E3Q1_HUMAN	BMP2	Bone morphogenetic protein 2	3	0.317011	0.10559	0.278341	0.051668
2	tr|K7EKD8|K7EKD8_HUMAN	SDF4	45 kDa calcium-binding protein	3	0.385897	0.051998	0.349369	0.049074
3	tr|Q8WUV3|Q8WUV3_HUMAN	CSRP1	Cysteine and glycine-rich protein 1	4	0.403368	0.067666	0.32749	0.047143
4	tr|H0Y7A7|H0Y7A7_HUMAN	NUCB1	Nucleobindin 1 variant	18	0.493801	8.39E-05	0.480406	0.000151
5	sp|Q9HAV7|GRPE1_HUMAN	CLU	Clusterin	63	0.518533	0.001495	0.480786	0.000236
6	sp|Q12841|FSTL1_HUMAN	FSTL1	Follistatin-related protein 1	11	0.526944	0.005066	0.591959	0.002263
7	sp|O75787|RENR_HUMAN	ATP6AP2	Renin receptor	8	0.564742	0.00759	0.616903	0.009215
8	sp|Q16270|IBP7_HUMAN	IGFBP7	Insulin-like growth factor-binding protein 7	36	0.568981	0.005411	0.525776	0.002737
9	sp|P20809|IL11_HUMAN	IL-11	Interleukin-11	3	0.579813	0.077419	0.579813	0.077419
10	sp|P04406|G3P_HUMAN	GAPDH	Glyceraldehyde-3-phosphate dehydrogenase	108	0.581235	0.001442	0.49832	2.85E-05
11	sp|P07339|CATD_HUMAN	CTSD	Cathepsin D	23	0.596307	0.011429	0.556281	0.005984
12	sp|P19022|CADH2_HUMAN	CDH2	Cadherin-2	10	0.597	0.029602	0.583355	0.045716
13	tr|Q5U000|Q5U000_HUMAN	CTSZ	Cathepsin Z	11	0.614062	0.04132	0.588521	0.004804
14	sp|Q13421|MSLN_HUMAN	MSLN	Mesothelin	63	0.619085	0.031075	0.643571	0.01251
15	tr|Q7Z3Z9|Q7Z3Z9_HUMAN	L1CAM	L1 cell adhesion molecule	42	0.620206	0.000147	0.604773	0.000235
16	sp|Q8NES3|LFNG_HUMAN	LFNG	β-1,3-N-acetylglucosaminyltransferase lunatic fringe	3	0.630394	0.003585	0.512136	0.00982
17	sp|P20827|EFNA1_HUMAN	EFNA1	Ephrin-A1	8	0.641523	0.038208	0.654235	0.0573
18	sp|P00966|ASSY_HUMAN	ASS1	Argininosuccinate synthase	62	0.652695	0.015085	0.635661	0.016378
19	sp|P35555|FBN1_HUMAN	FBN1	Fibrillin-1	23	0.676557	0.006903	0.736246	0.016766
20	sp|P17936|IBP3_HUMAN	IGFBP3	Insulin-like growth factor-binding protein 3	9	0.703906	0.005939	0.758705	0.01324
21	sp|P51884|LUM_HUMAN	LUM	Lumican	21	0.707534	0.007503	0.71794	5.66E-05
22	sp|P16035|TIMP2_HUMAN	TIMP2	Metalloproteinase inhibitor 2	15	0.717572	0.036572	0.683828	0.037238
23	tr|Q2M1J3|Q2M1J3_HUMAN	ROBO1	ROBO1 protein	16	0.717682	0.005528	0.71049	0.014984
24	sp|P28799|GRN_HUMAN	GRN	Granulins	13	0.718265	0.042939	0.644782	0.013296
25	sp|Q9H4F8|SMOC1_HUMAN	SMOC1	SPARC-related modular calcium-binding protein 1	16	0.727941	0.035403	0.708092	0.011316
26	sp|P24752|THIL_HUMAN	ACAT1	Acetyl-CoA acetyltransferase, mitochondrial	6	0.732777	0.045963	0.709778	0.042653
27	sp|P10809|CH60_HUMAN	HSPD1	60 kDa heat shock protein, mitochondrial	24	0.73754	0.007491	0.636544	0.000373
28	sp|P05067|A4_HUMAN	APP	Amyloid β A4 protein	18	0.741021	0.01009	0.716255	0.020473
29	sp|Q92626|PXDN_HUMAN	PXDN	Peroxidasin homolog	51	0.746291	0.000592	0.747293	0.001493
30	sp|Q9BRK5|CAB45_HUMAN	COL1A1	Collagen α-1(I) chain	5	0.753276	0.020072	0.447282	0.011558

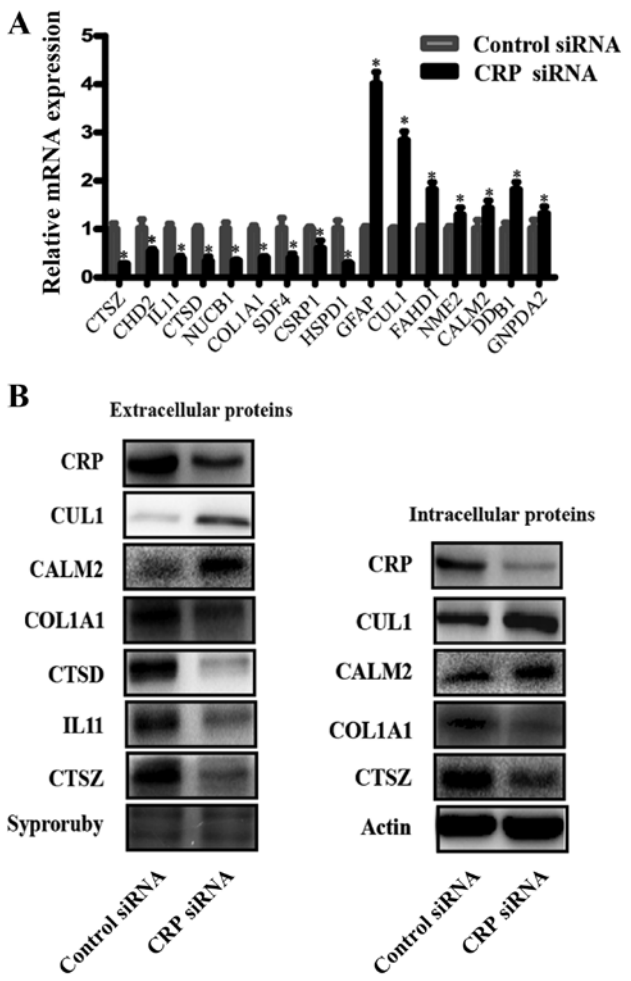

Figure 4. Verification of the differentially expressed proteins. (A) Real-time RT-PCR detected the relative mRNA expression levels of CTSZ, CDH2, IL11, CTSD, NUCB1, COL1A1, SDF4, CSRP1, HSPD1, GFAP, CUL1, FAHD1, NME2, CALM2, DDB1 and GNPDA2, as normalized to GADPH (*P<0.05). (B) A representative western blot analysis for CTSZ, IL11, CTSD, COL1A1 CUL1 and CALM2 expression in intracellular and extracellular samples from HepG2 lines. (Bars indicate SD, *P<0.05). Actin was used as the normalization standard.

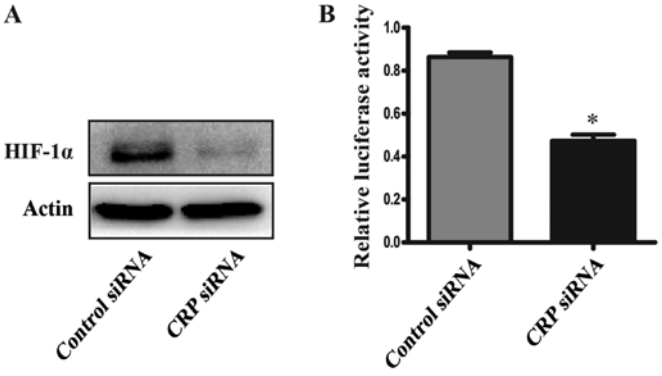

Figure 5. CRP knockdown reduced the production and luciferase activity of HIF-1α in HepG2 lines. (Bars indicate SD, *P<0.05). Actin was used as the normalization standard.

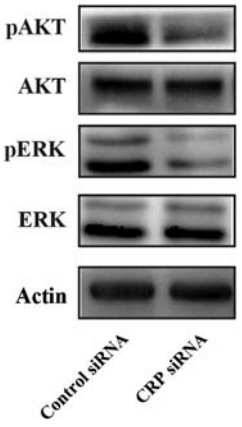

Figure 6. CRP knockdown inhibited phosphorylation of ERK and Akt in HepG2 lines.

siRNA-treated samples. The trend was consistent with the results of the iTRAQ approach. In order to validate the levels of several proteins, western blot analyses were performed. Fig. 4B shows the western blot analysis results of CTSZ, IL11, CTSD, COL1A1 CUL1 and CALM2 expression in intracellular and extracellular samples. Supernatant protein from CRP siRNA-treated cells had obviously decreased expression levels of CTSZ, IL11, CTSD, COL1A1 and increased expression levels of CUL1 and CALM2, compared to negative control siRNA-treated cells. IL11 and CTSD are, intracellularly, low expression proteins, thus, these were not detected in the western blot analyses. In addition to these two proteins, other proteins are similarly expressed intracellularly.

CRP knockdown downregulates HIF-1α expression and the luciferase activity of HIF-1α in HepG2 cells. Because CRP could affect the activity of HIF-1α, which has also been shown to induce expression of CTSD (21). CTSD accociated with the growth, proliferation and metastasis of tumors (22). The expression and luciferase activity of HIF-1α was determined using the western blot analyses and Dual-luciferase reporter assay system. Our results showed that the expression and luciferase activity of HIF-1α was significantly reduced in CRP siRNA treated HepG2 cells, compared to the control group (Fig. 5).

CRP knockdown suppresses ERK and Akt phosphorylation in HepG2 cells. MEK/ERK and PI3K/AKT signaling pathways play important roles in migration, invasion and metastasis of cancer (23). CRP could upregulate VEGF-A expression via the MEK/ERK and PI3K/AKT signaling pathways in adipose-derived stem cells (24). We hypothesize that CRP promotes migration, invasion, and metastasis of HCC through MEK/ERK and PI3K/AKT signaling pathways. We observed that the downregulation of CRP remarkably inhibits ERK and Akt phosphorylation at the protein level when compared to control siRNA in HepG2 cells (Fig. 6). These results indicate that CRP may induce cell migration, and invasion through MEK/ERK and PI3K/AKT signaling pathways.

Discussion

Using proteomic strategies, a growing body of evidence has identified proteins specifically upregulated or downregulated in HCC tissues that can be considered as early diagnostic markers, prognostic markers and therapeutic targets (25,26).

CRP is such a protein overexpressed in various types of tumors (6-10), and is a promising biomarker of HBV-related HCC (27). However, little is known about the function of CRP in HCC cells.

The present study demonstrates that CRP was significantly overexpressed in HCC tissues compared to non-cancerous tissues. Extra-hepatic metastases of HCC, which is the main cause of cancer-related death, depend largely on the migratory and invasive capabilities of HCC cells. Several studies have demonstrated that CRP promoted cell proliferation in endothelial cells, endothelial progenitor cells, renal tubular epithelial cells and provided protection from apoptosis in myeloma cells, *in vitro* and *in vivo* (11,12). Here, we demonstrated that CRP knockdown in HepG2 and BEL7402 cells significantly suppressed cell growth, migration and invasion *in vitro*, as shown in wound assays and Transwell assays. Our findings provide the first piece of evidence that CRP silencing inhibited migration and invasion, suggesting a carcinogenic role for CRP in HCC.

To investigate the potential molecular mechanism by which CRP contributes to migration and invasion, iTRAQ-based MS was performed to analyze secretory DEPs between CRP siRNA-treated and negative siRNA-treated HepG2 cells. Our iTRAQ analysis identified 109 aberrantly expressed proteins in CRP siRNA-treated samples. Many of them, including CTSZ, IL11, CTSD, COL1A1, CUL1 and CALM2, were identified using western blot analysis and RT-PCR analyses. The data indicated that the iTRAQ technology is both reliable and powerful for protein quantification. Among these proteins, we focused on cathepsin D (CTSD) because the expression of CTSD was obviously downregulated in CRP siRNA-treated samples, compared to control negative siRNA-treated samples, and is closely associated with invasion and metastasis of cancer cells.

Cathepsin D, a member of the aspartic proteinase superfamily in the lysosomes of eukaryotic cells (28), degrades the extracellular matrix (ECM) and is overexpressed and hypersecreted by carcinoma cells (29). Accumulated data show that CTSD is secrected in breast, prostate, ovaria, and lung cancer cell lines, and acts as a autocrine cancer cell growth factor involving cancer development (30). In addition, CTSD correlates with poor prognoses, invasion and metastasis in many malignancies (22,31,32). Several possible mechanisms have been proposed. For instance, CTSD promotes angiogenesis by releasing basic fibroblast growth factor (33). Additionally, CTSD can degrade anti-angiogenesis growth factors, such as angiogenesis inhibitor 16K prolactin and endostatin (34). HIF1, a transcription factor, is one of the important players in modulation of cell metabolism and plays an essential role in cellular and systemic homeostatic responses to hypoxia. HIF-1α in itself induces expression of several glycolytic enzymes, as well as inhibits entry into the TCA-cycle (35). Several studies have shown that high expression of HIF-1α correlated with a short survival in non-small cell lung cancer (NSCLC) (36-38). HIF-1α has also been shown to induce expression ofCTSD (21). Based on the close relationship between HIF-1α and CTSD, and the observation that CTSD was significantly decreased when CRP was silenced. We further measured expression and activity of HIF-1α. Our result showed that expression and luciferase activity of HIF-1α was decreased in CRP siRNA treated HepG2 cells. Thus, we hypothesized that when silencing CRP, the decrease in CTSD may be through this pathway.

It has been reported that activation of MEK/ERK and PI3K/AKT signaling pathways play important roles in migration, invasion and metastasis of cancer (23). CRP could upregulate VEGF-A expression by activating HIF-1α via the MEK/ERK and PI3K/AKT signaling pathways in adipose-derived stem cells (ADSCs) (24). However, few studies have reported on the relationship of CRP and MEK/ERK and PI3K/AKT signaling pathways in HCC. Therefore, we investigated whether CRP was capable of promoting migration, invasion via the MEK/ERK and PI3K/AKT pathway in HCC cells. Our results showed that CRP knockdown remarkably inhibits ERK and Akt phosphorylation at the protein level when compared to control siRNA in HepG2 cells. Therefore, our data support that activation of MEK/ERK and PI3K/AKT signaling pathways may required for CRP-stimulated cell migration and invasion of HCC cells.

In conclusion, we have demonstrated that CRP is highly expressed in tumor tissues and promotes invasion and metastases in HCC cell lines. In addition, we have performed a quantitative proteomic profiling of supernatant proteins from CRP siRNA-treated and negative control siRNA-treated HepG2 cells. We observed 109 aberrantly expressed proteins in CRP siRNA-treated samples. Moreover, silencing of CRP abrogates HIF-1α expression levels, the luciferase activity of HIF-1α, and ERK and Akt phosphorylation in HepG2 cells. The present study provides a novel mechanism by which CRP promotes the proliferation, migration, invasion, metastasis of hepatocellular carcinoma cells. Inhibition of CRP could suppress migration, invasion and healing of hepatoma carcinoma cells by decreasing HIF-1α activity and CTSD.

Acknowledgements

The present study was supported by the National Natural Science Foundation of China (81171560), the National Key Technology Support Program (2012BAI35B03), the 'Par-Eu Scholars Program' of Chongqing City, the National Science and Technology Major Project of China (2012ZX10002007001), the Chongqing Natural Science Foundation, the Chongqing Municipal Science and Technology (no. cstc2012jjA10064), and the Natural Science Foundation Project of CQ CSTC (2013jcyjA10060).

References

1. El-Serag HB: Epidemiology of viral hepatitis and hepatocellular carcinoma. Gastroenterology 142: 1264-1273.e1, 2012.
2. El-Serag HB and Kanwal F: Epidemiology of hepatocellular carcinoma in the United States: Where are we? Where do we go? Hepatology 60: 1767-1775, 2014.
3. Ren W, Qi X, Jia J, Yang M and Han G: Hepatocellular carcinoma. Lancet (London, England) 380: 469; author reply 470-461, 2012.
4. Stein MP, Edberg JC, Kimberly RP, Mangan EK, Bharadwaj D, Mold C and Du Clos TW: C-reactive protein binding to FcgammaRIIa on human monocytes and neutrophils is allele-specific. J Clin Invest 105: 369-376, 2000.
5. Pepys MB: C-reactive protein: The role of an ancient protein in modern rheumatology. Clin Exp Rheumatol 1: 3-7, 1983.
6. Hefler LA, Concin N, Hofstetter G, Marth C, Mustea A, Sehouli J, Zeillinger R, Leipold H, Lass H, Grimm C, *et al*: Serum C-reactive protein as independent prognostic variable in patients with ovarian cancer. Clin Cancer Res 14: 710-714, 2008.

7. Xu M, Zhu M, Du Y, Yan B, Wang Q, Wang C and Zhao J: Serum C-reactive protein and risk of lung cancer: A case-control study. Med Oncol 30: 319, 2013.
8. Chung YC and Chang YF: Serum C-reactive protein correlates with survival in colorectal cancer patients but is not an independent prognostic indicator. Eur J Gastroenterol Hepatol 15: 369-373, 2003.
9. Bataille R, Boccadoro M, Klein B, Durie B and Pileri A: C-reactive protein and beta-2 microglobulin produce a simple and powerful myeloma staging system. Blood 80: 733-737, 1992.
10. Legouffe E, Rodriguez C, Picot MC, Richard B, Klein B, Rossi JF and Commes T: C-reactive protein serum level is a valuable and simple prognostic marker in non Hodgkin's lymphoma. Leuk Lymphoma 31: 351-357, 1998.
11. Yang J, Wezeman M, Zhang X, Lin P, Wang M, Qian J, Wan B, Kwak LW, Yu L and Yi Q: Human C-reactive protein binds activating Fcgamma receptors and protects myeloma tumor cells from apoptosis. Cancer Cell 12: 252-265, 2007.
12. Liu F, Chen HY, Huang XR, Chung AC, Zhou L, Fu P, Szalai AJ and Lan HY: C-reactive protein promotes diabetic kidney disease in a mouse model of type 1 diabetes. Diabetologia 54: 2713-2723, 2011.
13. Ho J, Kong JW, Choong LY, Loh MC, Toy W, Chong PK, Wong CH, Wong CY, Shah N and Lim YP: Novel breast cancer metastasis-associated proteins. J Proteome Res 8: 583-594, 2009.
14. Hu H, Ding X, Yang Y, Zhang H, Li H, Tong S, An X, Zhong Q, Liu X, Ma L, *et al*: Changes in glucose-6-phosphate dehydrogenase expression results in altered behavior of HBV-associated liver cancer cells. Am J Physiol Gastrointest Liver Physiol 307: G611-G622, 2014.
15. Ran X, Xu X, Yang Y, She S, Yang M, Li S, Peng H, Ding X, Hu H, Hu P, *et al*: A quantitative proteomics study on olfactomedin 4 in the development of gastric cancer. Int J Oncol 47: 1932-1944, 2015.
16. Wang LN, Tong SW, Hu HD, Ye F, Li SL, Ren H, Zhang DZ, Xiang R and Yang YX: Quantitative proteome analysis of ovarian cancer tissues using a iTRAQ approach. J Cell Biochem 113: 3762-3772, 2012.
17. Yang Y, Toy W, Choong LY, Hou P, Ashktorab H, Smoot DT, Yeoh KG and Lim YP: Discovery of SLC3A2 cell membrane protein as a potential gastric cancer biomarker: Implications in molecular imaging. J Proteome Res 11: 5736-5747, 2012.
18. Livak KJ and Schmittgen TD: Analysis of relative gene expression data using real-time quantitative PCR and the 2(-Delta Delta C(T)) method. Methods 25: 402-408, 2001.
19. Gan CS, Chong PK, Pham TK and Wright PC: Technical, experimental, and biological variations in isobaric tags for relative and absolute quantitation (iTRAQ). J Proteome Res 6: 821-827, 2007.
20. Zhou C, Simpson KL, Lancashire LJ, Walker MJ, Dawson MJ, Unwin RD, Rembielak A, Price P, West C, Dive C, *et al*: Statistical considerations of optimal study design for human plasma proteomics and biomarker discovery. J Proteome Res 11: 2103-2113, 2012.
21. Krishnamachary B, Berg-Dixon S, Kelly B, Agani F, Feldser D, Ferreira G, Iyer N, LaRusch J, Pak B, Taghavi P, *et al*: Regulation of colon carcinoma cell invasion by hypoxia-inducible factor 1. Cancer Res 63: 1138-1143, 2003.
22. Dian D, Heublein S, Wiest I, Barthell L, Friese K and Jeschke U: Significance of the tumor protease cathepsin D for the biology of breast cancer. Histol Histopathol 29: 433-438, 2014.
23. Yoo YA, Kang MH, Lee HJ, Kim BH, Park JK, Kim HK, Kim JS and Oh SC: Sonic hedgehog pathway promotes metastasis and lymphangiogenesis via activation of Akt, EMT, and MMP-9 pathway in gastric cancer. Cancer Res 71: 7061-7070, 2011.
24. Chen J, Gu Z, Wu M, Yang Y, Zhang J, Ou J, Zuo Z, Wang J and Chen Y: C-reactive protein can upregulate VEGF expression to promote ADSC-induced angiogenesis by activating HIF-1α via CD64/PI3k/Akt and MAPK/ERK signaling pathways. Stem Cell Res Ther 7: 114, 2016.
25. Lee IN, Chen CH, Sheu JC, Lee HS, Huang GT, Chen DS, Yu CY, Wen CL, Lu FJ and Chow LP: Identification of complement C3a as a candidate biomarker in human chronic hepatitis C and HCV-related hepatocellular carcinoma using a proteomics approach. Proteomics 6: 2865-2873, 2006.
26. Feng JT, Liu YK, Song HY, Dai Z, Qin LX, Almofti MR, Fang CY, Lu HJ, Yang PY and Tang ZY: Heat-shock protein 27: A potential biomarker for hepatocellular carcinoma identified by serum proteome analysis. Proteomics 5: 4581-4588, 2005.
27. She S, Xiang Y, Yang M, Ding X, Liu X, Ma L, Liu Q, Liu B, Lu Z, Li S, *et al*: C-reactive protein is a biomarker of AFP-negative HBV-related hepatocellular carcinoma. Int J Oncol 47: 543-554, 2015.
28. Westley B and Rochefort H: A secreted glycoprotein induced by estrogen in human breast cancer cell lines. Cell 20: 353-362, 1980.
29. Rochefort H, Capony F, Garcia M, Cavaillès V, Freiss G, Chambon M, Morisset M and Vignon F: Estrogen-induced lysosomal proteases secreted by breast cancer cells: A role in carcinogenesis? J Cell Biochem 35: 17-29, 1987.
30. Berchem G, Glondu M, Gleizes M, Brouillet JP, Vignon F, Garcia M and Liaudet-Coopman E: Cathepsin-D affects multiple tumor progression steps in vivo: Proliferation, angiogenesis and apoptosis. Oncogene 21: 5951-5955, 2002.
31. Vashishta A, Ohri SS, Proctor M, Fusek M and Vetvicka V: Ribozyme-targeting procathepsin D and its effect on invasion and growth of breast cancer cells: An implication in breast cancer therapy. Int J Oncol 30: 1223-1230, 2007.
32. Glondu M, Liaudet-Coopman E, Derocq D, Platet N, Rochefort H and Garcia M: Down-regulation of cathepsin-D expression by antisense gene transfer inhibits tumor growth and experimental lung metastasis of human breast cancer cells. Oncogene 21: 5127-5134, 2002.
33. Briozzo P, Badet J, Capony F, Pieri I, Montcourrier P, Barritault D and Rochefort H: MCF7 mammary cancer cells respond to bFGF and internalize it following its release from extracellular matrix: A permissive role of cathepsin D. Exp Cell Res 194: 252-259, 1991.
34. Piwnica D, Fernandez I, Binart N, Touraine P, Kelly PA and Goffin V: A new mechanism for prolactin processing into 16K PRL by secreted cathepsin D. Mol Endocrinol 20: 3263-3278, 2006.
35. Keith B, Johnson RS and Simon MC: HIF1α and HIF2α: Sibling rivalry in hypoxic tumour growth and progression. Nat Rev Cancer 12: 9-22, 2011.
36. Hung JJ, Yang MH, Hsu HS, Hsu WH, Liu JS and Wu KJ: Prognostic significance of hypoxia-inducible factor-1alpha, TWIST1 and Snail expression in resectable non-small cell lung cancer. Thorax 64: 1082-1089, 2009.
37. Kim SJ, Rabbani ZN, Dewhirst MW, Vujaskovic Z, Vollmer RT, Schreiber EG, Oosterwijk E and Kelley MJ: Expression of HIF-1alpha, CA IX, VEGF, and MMP-9 in surgically resected non-small cell lung cancer. Lung Cancer 49: 325-335, 2005.
38. Giatromanolaki A, Koukourakis MI, Sivridis E, Turley H, Talks K, Pezzella F, Gatter KC and Harris AL: Relation of hypoxia inducible factor 1 alpha and 2 alpha in operable non-small cell lung cancer to angiogenic/molecular profile of tumours and survival. Br J Cancer 85: 881-890, 2001.